Proceedings of Ninth World Conference on Earthquake Engineering
August 2-9, 1988, Tokyo-Kyoto, JAPAN (Vol.VI)

10-4-6

DYNAMIC RESPONSE CHARACTERISTICS OF CYLINDRICAL LIQUID STORAGE TANKS WITH DEFORMABLE BOTTOM PLATE IN VERTICAL VIBRATION

Tadahiro FUKUSUMI[1], Hisashi NOZOE[2]
Yoshihisa GYOTEN[3] and Koji MIZUHATA[1]

[1]Faculty of Engineering, Kobe University, Nada-ku, Kobe, Japan
[2]Graduate School of Science and Technology, Kobe University, Nada-ku, Kobe, Japan
[3]Professor Emeritus, Kobe University, Nada-ku, Kobe Japan

SAMMARY

Cylindrical liquid storage tank of cantilevered type with flexible bottom plate supported on the surface of the soil layer and subjected to the harmonic vertical ground excitation is dealt with. Theoretical solutions of displacement and stress of the soil and tank are obtained. The influence of the rigidity of the plate and the soil layer on the dynamic response characteristics of the soil-tank system is discussed.

INTRODUCTION

A few studies pertinent to the dynamic response of flexible foundation have been presented recently, For rectangular plates on an elastic half space, Iguchi and Luco (Ref.1) obtained numerical results by use of the subdivision method which divides the contact region between the ground and the plate into small subregions, and reported on the influence of the flexibility of the plate on the impedance functions which differs from those of rigid plate. Similarly, Whittaker and Christiano (Ref.2) studied including the investigation on the effect of the mass of the plate. From the earthquake observations of the liquid storage tanks, predominance of the axisymmetrical mode have been sometimes reported. This paper is adressed to the study of the axisymmetrical response of the cylindrical liquid storage tank with deformable bottom plate supported on a soil layer under the harmonic and vertical excitation. By employing the finite Fourier-Hankel transformation method, theoretical solution can be obtained and numerical results describing the dynamic response characteristics are presented.

FORMULATION OF THE PROBLEM

The analysis model of the soil-tank system subjected to the harmonic vertical vibration is shown in Fig.1. The soil layer is dealt by dividing into two fields, i.e. near field I and far field II, by an imginary (transmitting) boundary at $r=R_0$. The tank consists of three parts, i.e. a flexible circular bottom plate, cylindrical shell wall and liquid, which are consistently dealt as continua. In the analysis the followings are assumed.

1. Soil layer is homogeneous, isotropic and resting on a rigid bedrock. In the far field, the horizontal component of the dilatational strain is neglected,
2. The bottom plate and the side wall of the tank are elastic,
3. At the interface (at z=H), contact condition of vertical displacement, i.e. $w_P=w_I$ at $r\leq r_0$ and frictionless condition, i.e. $\tau_{rzI}=0$ at $r\leq R_0$, are adopted,

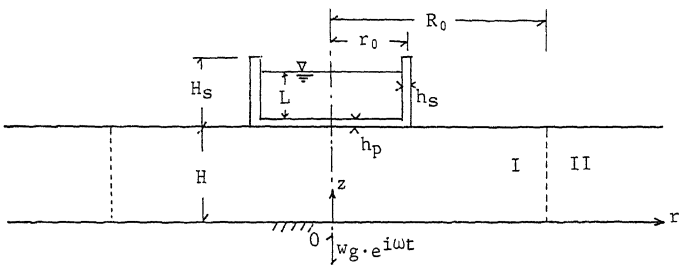

Fig. 1 Soil-Tank System in the Analysis

4. Hysteretic damping is assumed for the soil, bottom plate and side wall,
5. Liquid is incompressible, irrotational and inviscid.

Analysis of the Soil Layer The equation of motion of the soil layer subjected to the harmonic and vertical vibration is written as follows.

$$(\lambda+2\mu)\left[\frac{1}{r}(ru)'\right]' + \mu u'' + (\lambda+\mu)w'' + \rho\omega^2 u = 0 \ , \tag{1}$$

$$(\lambda+2\mu)w'' + \mu\frac{1}{r}(rw')' + (\lambda+\mu)\left[\frac{1}{r}(ru)'\right]' + \rho\omega^2(w+w_g) = 0 \ , \tag{2}$$

where u and w are the horizontal and vertical relative displacements in the r and the z directions in Fig.1, w_g is the amplitude of the vertical motion at the bedrock, time factor $e^{i\omega t}$ is omitted for convenience. $F'=\partial F/\partial r$ and $F'=\partial F/\partial z$. By introducing the fraction of the linear hysteretic damping ξ, Lame's constants λ and μ in Eqs.(1) and (2) are expressed as

$$\lambda = (1 + \xi i)\lambda_0, \quad \mu = (1 + \xi i)\mu_0 \ . \tag{3}$$

For near field I, by the finite Hankel transformation of the first order in the r direction and the finite Fourier cosine transformation in the z direction of Eq.(1) and similarly by the finite Hankel transformation of order zero and the finite Fourier sine transformation of Eq.(2), i.e. by operating Eqs.(1) and (2) as

$$\int_0^H\int_0^{R_0}\{\text{Eq.(1)}\}J_1(\beta_n r)r\,dr\cdot\cos\alpha_m z\,dz, \qquad \int_0^H\int_0^{R_0}\{\text{Eq.(2)}\}J_0(\beta_n r)r\,dr\cdot\sin\alpha_m z\,dz,$$

the differential equations (1) and (2) become a set of linear simultaneous equations in terms of imaginary functions $u_I^{1c}(\beta_n,\alpha_m)$ and $w_I^{0s}(\beta_n,\alpha_m)$ as follows.

$$\begin{bmatrix} (\lambda+2\mu)\beta_n^2+\mu\alpha_m^2-\rho\omega^2, & (\lambda+\mu)\beta_n\alpha_m \\ (\lambda+\mu)\beta_n\alpha_m, & (\lambda+2\mu)\alpha_m^2+\mu\beta_n^2-\rho\omega^2 \end{bmatrix} \begin{Bmatrix} u_I^{1c}(\beta_n,\alpha_m) \\ w_I^{0s}(\beta_n,\alpha_m) \end{Bmatrix} = \begin{Bmatrix} R_I^{1c}(\beta_n,\alpha_m) \\ Z_I^{0s}(\beta_n,\alpha_m) \end{Bmatrix} \ . \tag{4}$$

where $\alpha_m=(2m-1)\pi/2H$, β_n take zero (for n=0) and positive roots of $J_1(\beta_n R_0)=0$ (for n=1,2,..). The right side terms of the Eq.(4) include six imaginary functions which are dealt as the unknown constants. By the inverse transformation, the solutions of u_I and w_I are given in the following Fourier-Bessel series.

$$u_I(r,z) = \frac{2}{H}\sum_n\sum_m \frac{1}{N_n}u_I^{1c}(\beta_n,\alpha_m)\cdot\cos\alpha_m z\cdot J_1(\beta_n r), \tag{5}$$

$$w_I(r,z) = \frac{2}{H}\sum_m \left\{\frac{1}{N_0}w_I^{0s}(\bar{0},\alpha_m) + \sum_n \frac{1}{N_n}w_I^{0s}(\beta_n,\alpha_m)J_0(\beta_n r)\right\}\sin\alpha_m z \ , \tag{6}$$

where $N_n = R_0^2\{J_0(\beta_n R_0)\}^2/2$

For far field II, in accordance with the assumption that the horizontal component of the dilatational strain is neglected, the following equation instead of Eq.(1) is solved.

$$\frac{1}{r}(r u)' = 0 \ . \tag{7}$$

The solution of the horizontal displacement in the r direction u_{II} is given as

$$u_{II}(r,z) = \frac{1}{r}u_z(z) = \frac{1}{r}\cdot\frac{2}{H}\sum_m u_z^c(\alpha_m)\cos\alpha_m z \ , \tag{8}$$

where $u_z^c(\alpha_m)$ is an unknown constant. In Eq.(2), under the consideration of Eq.(7) and the following boundary conditions that

1. the vertical displacement w_{II} is zero at the base (at z=0),
2. w_{II} converges to zero as distance r tends to infinity,
3. normal stress σ_z in the vertical direction is zero at the surface of the soil layer (at z=H),

the solution is obtained as follows.

$$w_{II}(r,z) = \frac{2}{H}\sum_m \{\frac{K_0(q_m r)}{K_0(q_m R_0)}w_m + \frac{w_g}{\alpha_m}\cdot\frac{K_V^2}{\alpha_m^2 - K_V^2}\}\sin\alpha_m z \ , \tag{9}$$

where $q_m^2 = (\alpha_m^2 - K_V^2)\cdot(\lambda+2\mu)/\mu$, $K_V = \rho\omega^2/(\lambda+2\mu)$ and w_m is an unknown constant. Concerning to the soil layer, nine unknown constants are included.

Analysis of the tank Similar to the solution of the soil layer, the theoretical solution of the elastic circular plate, cylindrical shell wall and liquid are obtained in the form of the Fourier and Bessel series.

The equation of motion of the plate which is subjected to the liquid pressure p_p and the contact stress σ_0 of the soil layer is written as follows.

$$\nabla^2\nabla^2 w_p = \frac{1}{D_p}\{\rho_p h_p\omega^2(w_p+w_g) + p_p - \sigma_0\} \ , \tag{10}$$

where Dp is the flexural rigidity ; $D_p = (1+\xi_p\cdot i)E_p h_p^3/12(1-\nu_p^2)$. The relative displacement wp of the plate is expressed as

$$w_p(r) = \frac{1}{N_0}w_p^0(\bar{0}) + \sum_\ell \frac{1}{N_\ell}w_p^0(\gamma_\ell)\cdot J_0(\gamma_\ell r) \ , \tag{11}$$

where γ_ℓ take zero (for n=0) and positive roots of $J_1(\gamma_\ell R_0)=0$, $N_\ell = r_0^2\{J_0(\gamma_\ell R_0)\}^2/2$

The equations of motion of the shell in the radial and the vertical directions are

$$-\frac{B_s}{r_0^2}(\nu_s r_0 w_s' + u_s) - D_s u_s'''' + \rho_s h_s\omega^2 u_s + p_s = 0 \ , \tag{12}$$

$$\frac{B_s}{r_0}(r_0 w_s'' + \nu u_s') + \rho_s h_s\omega^2(w_s+w_g) = 0 \ , \tag{13}$$

where p_s is the liquid pressure, $B_s = (1+\xi_s\cdot i)\cdot E_s h_s/(1-\nu^2)$ and $D_s = B_s\cdot h_s^2/12$. The solutions of the horizontal and vertical relative displacements u_s and w_s of the shell are expressed as

$$u_s(z) = \frac{1}{H_S}\{u_s^c(\bar{0}) + 2\sum_j u_s^c(\alpha_j)\cos\alpha_j z\}, \tag{14}$$

$$w_s(z) = \frac{2}{H_s}\sum_j w_s^s(\alpha_j)\sin\alpha_j z \ , \tag{15}$$

where $\alpha_j = j\pi/H_s$.

Under the assumption of the ideal liquid, Laplace's equation given in terms of potential function ϕ becomes the governing equation. The solution is obtained in the similar form of the soil layer I and is expressed in terms of ϕ^{0c}.

The imaginary functions (w_p^0, u_s^c, w_s^s and ϕ^{0c}) of the plate, shell and liquid include 13 unknown constants. All the 22 unknown constants of the soil layer and the tank can be determined by solving a set of simultaneous equations.

NUMERICAL RESULTS AND DISCUSSION

The soil layer subjected to the uniform excitation $q_0 \cdot e^{i\omega t}$ (at z=H, $r \leq r_0$) is described first. The frequency response curves of vertical displacement, $wr_0\mu/P$ versus a_0, (w is average response in $r \leqq r_0$, $P = q_0 \cdot \pi r_0^2$ and a_0 is the non dimensional frequency of $a_0 = r_0 \cdot \omega / Vs$) are shown in Fig.2. (where $\nu=1/4$ and $H/r_0=2$) Difference of the results due to the different positions of the imaginary boundary (R_0/r_0 = 3, 4, 6 and 10) may be seen. Considering that converged results are obtained when larger value is taken as R_0/r_0 = 6 and 10, R_0/r_0 = 10 is taken in what follows. For a case of uniform excitation in a square zone (2Bx2B), comparing the compliance function (obtained by taking equivalent radius of $2B/\sqrt{\pi}$) with the others in Ref.3, this analysis method is confirmed to be valid.

Flexible plate subjected to the uniform excitation $q_0 \cdot e^{i\omega t}$ on the soil layer is discussed next. The distribution of the vertical displacement $\bar{w} = (w + wg)/wg$ and the contact stress σ_0 at the interface of the plate and the soil layer at different frequencies and flexural rigidity are shown in Figs. 3 and 4. (Concrete plate ; $Ep=2x10^6 t/m^2$, $\nu p=1/6$, $\rho p \cdot g=2.4t/m^3$, $\xi p=0.1$. Soil ; $\mu=9000t/m^2$, $\nu=1/3$, $\rho \cdot g=2t/m^3$, $\xi=0.2$). Where the results are obtained at the frequencies of b_1 = 1, 3.2 and 5 ($bi = f/f_1$, f_1 is the first natural frequency of the soil layer and $f_1 = Vp/4H$) for such a stiffness ratio of $Dp/\mu r_0^3$ = 2, 100, 500 ($x10^{-5}$) which corresponds to hp/r_0= 1, 3.7, 6.4 ($x10^{-2}$). As the frequency becomes high, it is observed that the displacement distribution becomes wavy. However, when the stiffness ratio is large, the wavy distribution tends to be smoothed and become uniform. Contact stress is shown in Fig.4. When the rigidity of the plate is very small, slight stresses are induced in the plate and the distribution of the contact stress retains almost the same to that of the excitation (uniform).

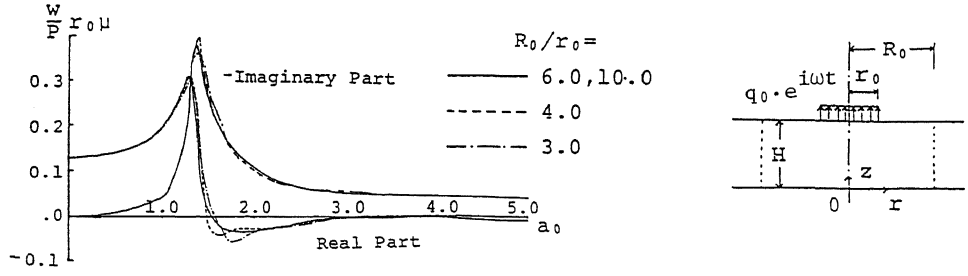

Fig. 2 Vretical Displacement Responses for Different R_0/r_0

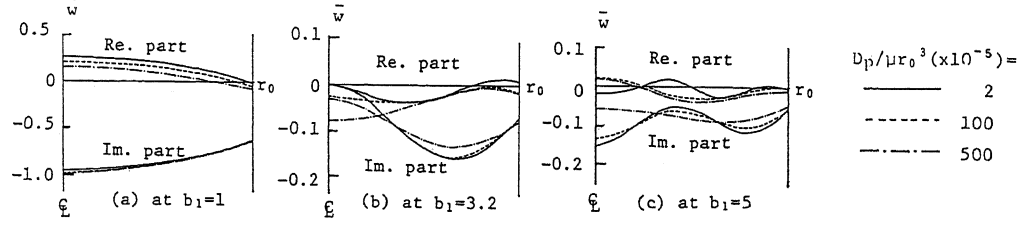

Fig. 3 Distribution of Vertical Displacement $\bar{w}$ for Different Stffness Ratio

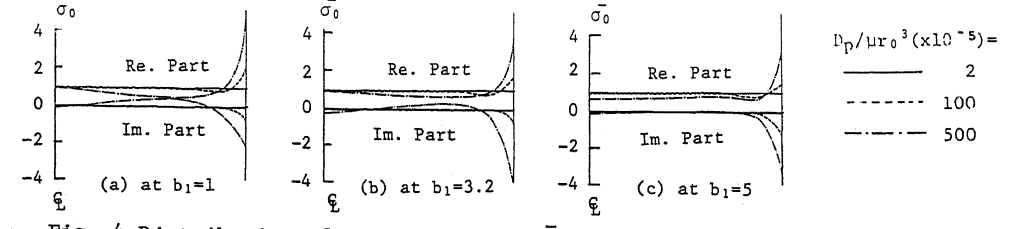

Fig. 4 Distribution of Contact Stress $\bar{\sigma_0}$ for Different Stiffness Ratio

While in case of relatively large stiffness ratio, contact stress is concentrated at the edge and the distribution approaches to Boussinesq's distribution obtained for the rigid plate.

Finally, the response of the soil-tank system subjected to the input excitation at the bedrock is discussed in comparison with the responses of free field and fixed tank (tank whose lower edge is clamped on the rigid base). Data in this analysis are as follows. Young's modulus of the tank (steel) : $Ep=Es = 2\times10^7 t/m^2$, thickness of the side wall : $hs/r_0 = 1/1000$ and the other data are tabulated in Table-1 and three cases of soil-tank system considered here are shown in Table-2.

Table-1 Data Used in the Analysis

		$\rho\cdot g(t/m^3)$	ν	ξ	dimension
soil		2.0	1/3	0.2	H/r_0 =2.0
Tank	plate	7.86	1/3	0.1	r_0/r_0=1.0
	wall	7.86	1/3	0.1	H_S/r_0=1.0
	liquid	1.0	-	-	L/r_0 =0.5

Table-2 Cases for Soil-Tank System

Case	$\mu(t/m^2)$	V_S(m/sec)	h_p/r_0
1	9000	210	1/1000
2	9000	210	1/100
3	2000	99	1/1000

Frequency response curves of the vertical displacement response at the surface of the soil layer are shown in Fig.5. In case of free field (Fig.5-a), resonant peaks appear at b_1 = 1, 3, 5. In cases 1, 2 and case 3 (Fig.5-b and 5-c), it is observed that the first resonant peak corresponding to the first natural frequency of the soil layer is maximum and the responses of amplitude and phase at the center and the edge (at r=0 and r_0) becomes different in higher frequency range of $b_1 > 1$. In cases 1 and 2, the second peak appears around at b_1 = 2.3 to 3.0 which corresponds to the first resonant frequency of horizontal displacement of the fixed tank (Fig. 6-a) and the second resonant frequency of the soil layer. In case 3 of softer ground (Vs = 99m/s), such a resonance is not appeared (around at b_1 = 4.6) in this figure.

Frequency response curves of the horizontal displacement $\bar{u}_S = u_S/w_g$ of the side wall of the tank near the lower edge (at z = Hs/10) are shown in Fig. 6-a (case of a fixed tank) and in Fig. 6-b (cases 1, 2 and 3). The first resonance of the cases 1, 2 and 3 corresponds to the first resonance of the vertical displacement of the soil layer. The second resonance of cases 1 and 2 corresponds to the resonance above mentioned, where the peak amplitude becomes smaller than that of the fixed tank, and the response of case 3 of softer ground is the

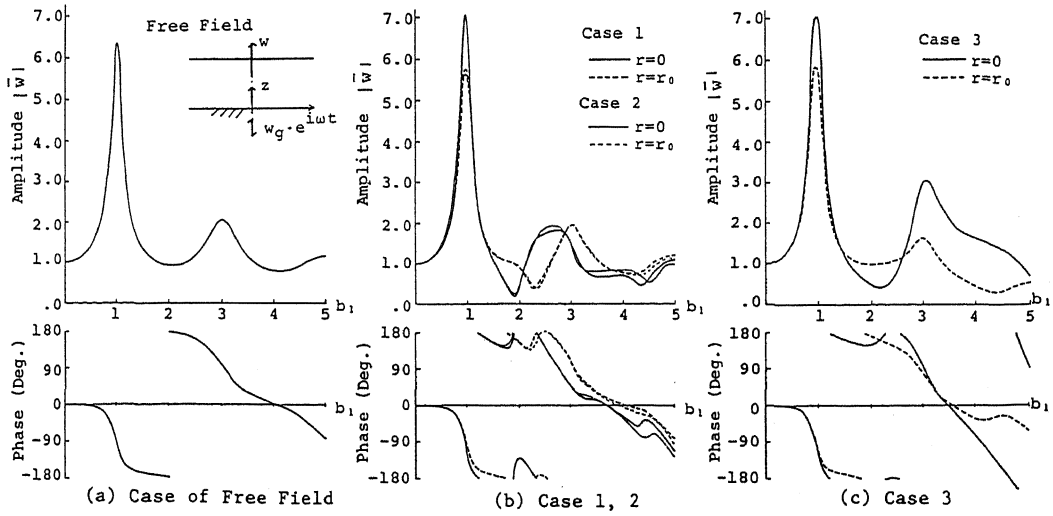

Fig. 5 Frequency Response Curves of Vertical Displacement $\bar{w}$

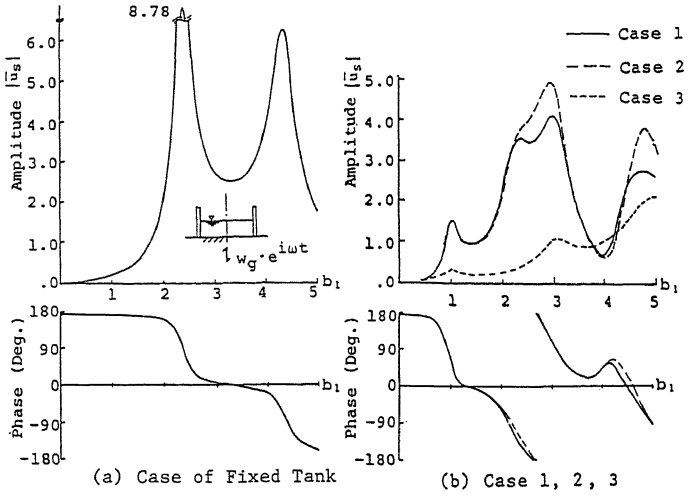

Fig. 6 Frequency Response Curves of Horizontal Displacement of the Side Wall of the Tank $\bar{u}_s$

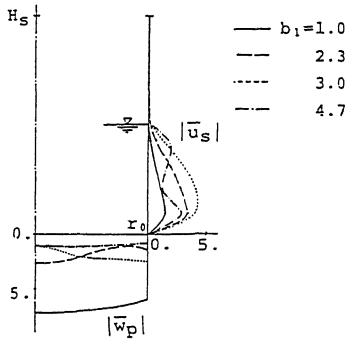

Fig.7 Distributions of Displacement Responses $|\bar{u}_s|$ and $|\bar{w}_p|$ at Different Frequencies (in Case 1)

smallest among these cases, which are suggested to be reduced by the effect of the radiation damping expected in $b_1 > 1$. Fig. 7 shows the distribution of the horizontal and vertical displacements $\bar{w}_p$ and $\bar{u}_s$ of the bottom plate and the side wall at four frequencies. Characteristic profile varied with frequency can be seen.

CONCLUSIONS

In the analysis, the soil layer is treated by dividing into two parts of near and far fields and the converged and accurate solution can be obtained when $R/r_0 \gtrsim 6$. From the numerical results of tanks with deformable bottom plate, the followings are observed. In case of the soil-tank system, both resonances of the free field and the fixed tank appear. Vertical displacement of the plate becomes maximum at the resonant frequency of the soil layer (at $b_1 = 1$) and at the higher frequency, the motion of the plate becomes different in phase and amplitude at each point. When the soil layer is relatively soft, the response of horizontal displacement of the side wall of the tank becomes small due to the effect of the radiation damping at higher frequency of $b_1 > 1$.

ACKNOWLEDGEMENTS

The authors wish to express their thanks to Dr. K. Kusakabe of Kobe University for his helpful advice and to Ms. A. Katabuki for her assistance.

REFERENCES

1. Iguchi, M. and Luco, J. E., "Dynamic Response of Flexible Rectangilar Foundations on an Elastic half-Space," Earthquake Eng. Struct. Dynamics, 9, 239-249, (1981).
2. Whittaker, W. L. and Christiano, P., "Dynamic Response of Plate on Elastic Half-Space," ASCE, 108, EM 1, Feb., 133-154, (1982).
3. Kobori, T, Minai, R. and Kusakabe, K, "Dynamic Characteristics of Soil-Structure cross interaction system," Bull. of Disaster Prevention Research Inst., Kyoto Univ., 22, (1973).